Experimental Determinations of Electron Inelastic Mean Free Paths in Silver, Gold, Copper and Silicon from Electron Elastic Peak Intensity Ratios

S. Tanuma, S. Ichimura[1], K. Goto [2], and T. Kimura

National Institute for Materials Science,1-2-1 Sengen, Tsukuba 305-0047 , Japan
[1]National Institute of Advanced Industrial Science and Technology , 1-1-4 Umezono, Tsukuba, Ibaraki 305-8568, Japan
[2]Nagoya Institute of Technology, Gokiso-chou, Showa-ku, Nagoya 466-8555, Japan

(Received February 8, 2002; accepted March 28, 2002)

We have determined inelastic mean free paths (IMFPs) in silver, gold , copper, and silicon in the 50 -5000 eV energy range from electron elastic peak intensity ratios to a nickel reference material, and Monte Carlo simulations. The resulting IMFPs were analyzed using Fano plots, and those values for silver, gold and copper could be fitted by the Bethe equation in the 50 – 5000 eV energy range. The resulting IMFPs for Ag, Au, Cu, and Si are in excellent agreement with IMFPs calculated from the Penn algorithm or the TPP-2M equation in the 200 - 5000 eV energy range.

1. Introduction

Electron inelastic mean paths (IMFPs), effective attenuation lengths (EALs), and escape depths (EDs) in solids are very important physical quantities for surface analyses by AES and XPS. The IMFP is the most basic parameter among them. Values of IMFPs could be determined from theoretical calculations [1] because reliable experimental determinations of the IMFP are a rather complicated task. Tanuma et al. calculated IMFPs for over 80 materials with the Penn algorithm [1] in the 50 – 2000 eV energy range and made clear their energy and material dependence [2-7].

The accuracy of IMFPs for a material depends in part on the accuracy of the used optical data (energy loss function) on which the calculation is based; this uncertainty is typically less than 10%, although it could be larger for some inorganic materials [3,4]. The other main source of inaccuracy is due to approximations in Penn algorithm. This uncertainty is believed to be about 10% for free-electron-like materials and for energies larger than 200 eV [2]. The uncertainty of IMFPs for other materials and at lower energies than 200 eV is expected to be larger but its magnitude is difficult to estimate. It is, then, very important to compare IMFPs calculated from theory with experimental values in order to check and know the reliability of the IMFPs.

Elastic peak electron spectroscopy is an efficient tool for experimental determination of IMFPs [8]. This method, usually, requires a reference specimen to obtain values of IMFPs but different values can be obtained according to the choice of the reference specimen [8]. We have here determined IMFPs of silver, gold, copper, and silicon using a Ni reference in the 50 - 5000 eV electron energy range.

2. Experimental

2.1 Measurement

The energy dependencies of the elastically backscattered primary electron current of nickel, gold, copper, silver, and silicon have been measured with a novel cylindrical analyzer (CMA) [9] in the 10 - 5000 eV range. The acceptance angle of the CMA is 42.3 ± 6 degree from the surface normal. Each elastic peak height was corrected for energy resolution and the EN (E) characteristics of the analyzer and normalized to the primary current (1 μA).

The specimens were polycrystals except for silicon, and were polished with alumina paste.

Before measurements, the specimen surface was cleaned by Ar^+ sputtering at 300 - 600 eV.

2.2 Calculation

Based on Monte Carlo calculations, the intensity of elastic scattered electrons can be described by the following equation.

$$\frac{I}{I_0} = F \times f_s \times \int_0^{\infty} \left(\frac{d\eta}{dS}\right) / N_0 \exp\left(-\frac{S}{\lambda}\right) dS \qquad \text{.....(1)}$$

Where F is a transmission efficiency of the CMA mesh, f_S is a surface excitation factor, $(d\eta/dS)$ is a histogram of the number of electrons versus total path length S of the elastically scattered electrons detected by the CMA, λ is the electron inelastic mean free path (IMFP) in a target material, and N_0 is the number of input electrons for the Monte Carlo calculation. In the calculations of differential elastic scattering cross section, the Thomas-Fermi-Dirac atomic potential was used for the elastic-scattering cross sections.

We have calculated elastically scattered electron intensities of Ag, Au, Cu, and Si in the 50 - 5000 eV energy range with the Monte Carlo method using the above equation. Since we need a very large number of random numbers (RNs) in the calculations, its generator plays an important role. We, then, used the Mersenne Twister which is a pseudo-random number generator developed by M. Matsumoto et al.[10]. It is proved that the period is $2^{19937-1}$, and the 623-dimensional equidistribution property is assured. We also used IMFP values of Ni in the 50 – 5000 eV energy range calculated from the Penn algorithm for the Monte Carlo calculations of elastic peak intensities[11].

The elastic intensity ratios of Ag, Au, Cu, and Si to the Ni reference can be expressed as

$$\frac{f_x \times \int_0^{\infty} \left(\frac{d\eta}{dS}\right)^X / N_0^X \exp\left(-\frac{S}{\lambda_X}\right) dS}{f_{Ni} \times \int_0^{\infty} \left(\frac{d\eta}{dS}\right)^{Ni} / N_0^{Ni} \exp\left(-\frac{S}{\lambda_{Ni}}\right) dS} - \frac{\left(\frac{I}{I_0}\right)^X_{measured}}{\left(\frac{I}{I_0}\right)^{Ni}_{measured}} = 0 \qquad \text{.....(2)}$$

where, λx means the IMFP for Ag, Au, Cu, and Si. If we suppose that the ratio of surface excitation correction factors is unity, the IMFP values can be determined by solving the above equation for λx; in this case the left hand term corresponds to the measured elastic peak intensity values.

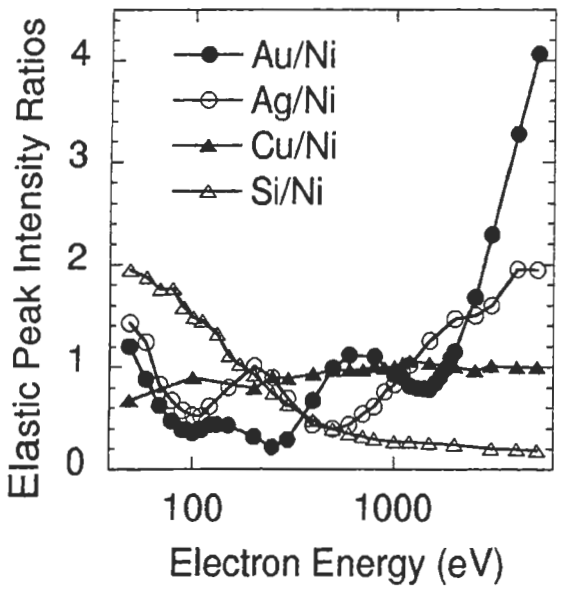

Figure 1. Measured elastic peak intensity ratios of Au, Ag, Cu and Si to a Ni-reference as a function of electron energy.

3. Results and Discussion

3.1 Energy dependence of elastic peak intensity ratios

The measured elastic-peak intensity ratios of Ag, Au, Cu, and Si to the Ni-reference are shown in Fig.1 as a function of electron energy. From this figure, we can see that the energy dependence of elastic peak intensity ratios are substantially different from element to element. These differences are attributed to the detailed differences in the elastic scattering behavior of each element, as represented by their differential elastic cross sections.

For Si, the intensity ratios monotonically decreased with increase electron energy; the ratios changed from 2 to 0.2. On the other

hand, the elastic-peak intensity ratios of Cu were almost constant (about 0.7-1.0) for all measured energies. Because the atomic number and electronic structure of Cu resemble that of the Ni-reference, they show the almost the same elastic scattering distribution. The energy dependence of Ag was different from those of Si and Cu, and has a complicated shape. The intensity ratios of Ag to Ni increased with increase of electron energy over 500 eV, with the ratios changing from 0.4 to 2.0. Under 500 eV, the Ag/Ni intensity showed a local maximum at around 200 eV and increased with decrease of electron energy. The results for Au also showed a complicated energy dependence, and resembled that of Ag. However, the range of the ratios are larger than those for Ag/Ni; the Au/Ni ratios changed from 0.2 to over 4.0.

3.2 IMFPs determined from elastic peak intensity ratios

The IMFPs of Ag, Au, Cu, and Si were determined from the ratios of the measured intensities of the elastic peaks to those of the Ni reference using equation (2). The IMFPs of Ni used in equation (2) were calculated from the Penn algorithm [1] as noted above. The parameters λx were obtained by solving equation (2) for λx of each material using the Ni IMFPs and the measured elastic peak intensities and by assuming $f_x = f_{Ni}$.

The resulting IMFPs of Ag, Au, Cu, and Si are shown in Figs. 2 - 5,s respectively. In Figs. 2 and 4, the resulting IMFPs of Ag and Cu are in excellent agreement with those from the Penn algorithm and from the TPP-2M equation [6] over the 50 - 5000 eV energy range. Figure 3 shows that the IMFPs for Au coincide well with those from the Penn algorithm and from the TPP-2M equation over the 200 - 5000 eV energy range. We thus conclude that the IMFP ratios of Au, Ag and Cu to the Ni reference, which are calculated from the Penn algorithm and from the TPP-2M, are quite accurate in the 200 - 5000 eV range. Furthermore, these experimental results indicate that the surface excitation factors f_S for Ag, Cu and Ni have the same magnitude and the same energy dependence over the 50 - 5000 eV range. But f_S for Au is different from that of Ni for energies less than 200 eV.

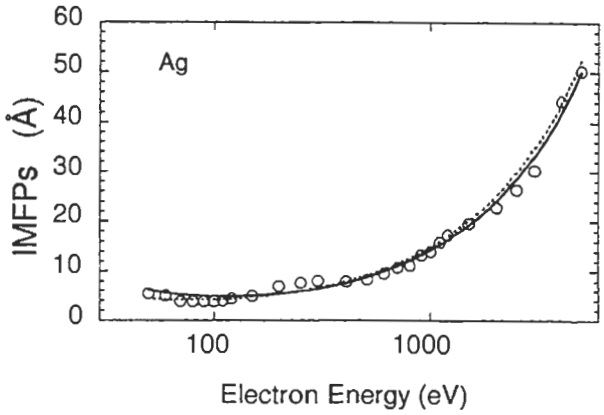

Figure 2. IMFP values (open circles) determined from elastic peak intensity ratios for silver as a function of electron energy. The solid line shows IMFP values calculated from the Penn algorithm using the energy loss function from optical data. The dotted line shows IMFPs calculated from the predictive formula TPP-2M.

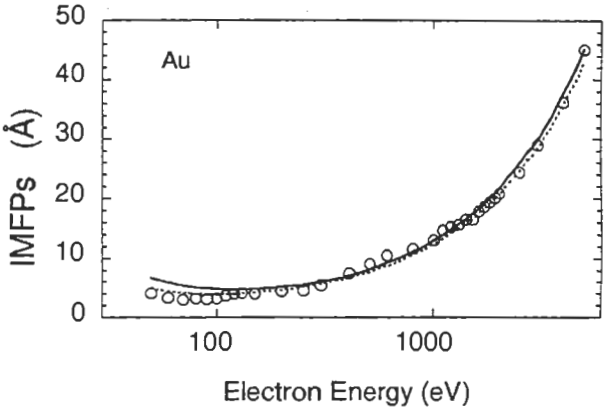

Figure 3. IMFP results for gold as a function of electron energy; see caption to Fig. 2.

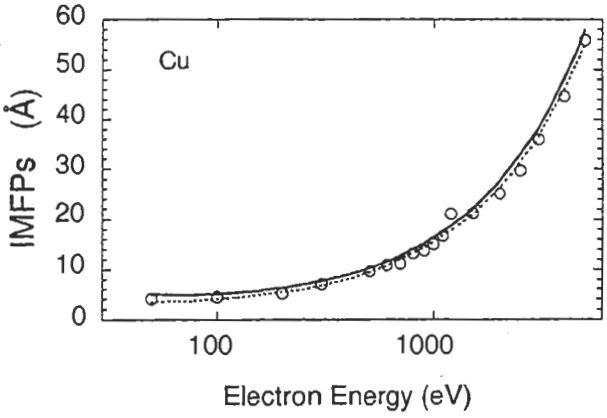

Figure 4. IMFP results for copper as a function of electron energy; see caption to Fig. 2.

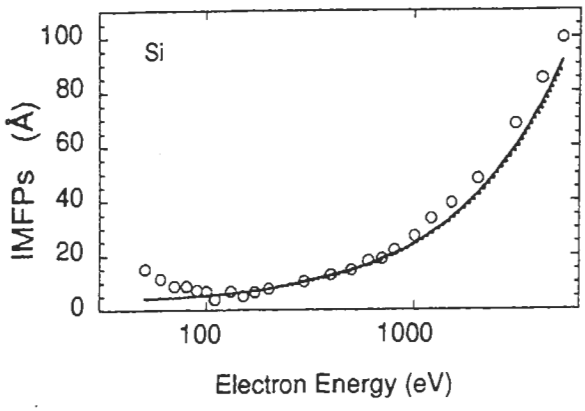

Figure 5. IMFP results for silicon as a function of electron energy; see caption to Fig. 2.

On the other hand, figure 5 show the IMFPs for Si determined from elastic-peak intensity ratios together with those from theoretical calculations. The measured IMFPs for Si coincide well with those from the Penn algorithm and from TPP-2M in the 100 - 1000 eV range. Over 1000 eV, the measured IMFPs are, however, larger than those from the theoretical calculations. One reason might be due to the crystalline nature of the Si specimen because single crystal silicon was used for the experiments (although the surface was sputtered by Ar^+ at 250 - 300 eV). We also point out that the surface correction factor fs for Si is different from that of Ni in magnitude and in its energy dependence because Si is a typical free-electron-like material and Ni is a typical transition metal. This factor might account for the deviations below 100 eV.

However, in the 100 - 5000 eV region the energy dependence of the measured IMFPs for Si resemble those from TPP-2M (or from the Penn algorithm).

3.3 Analysis of resulting IMFPs with Fano plots

We have analyzed experimentally determined IMFPs in Figs. 2-5 using Fano Plots which were constructed by plotting values of E/λ *versus* ln E. The Fano plots for Au, Ag, Cu and Si are shown in Fig. 6. Since the data points lie sufficiently close to straight lines, values of the parameters in the simple Bethe formula are

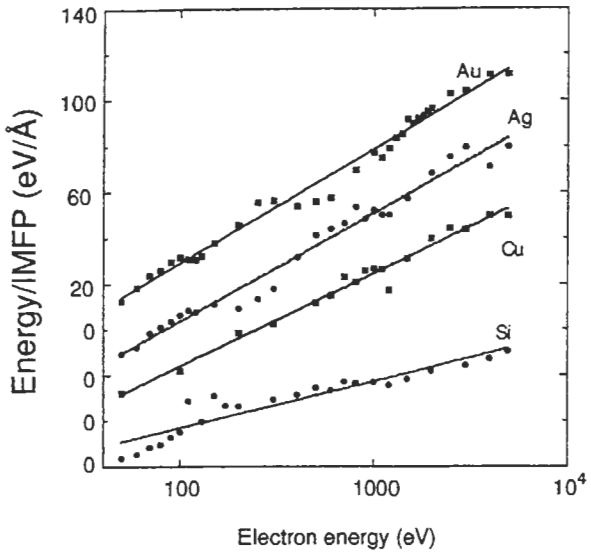

Figure 6. Fano plots (solid symbols) of silver, gold, copper and silicon calculated from experimentally determined IMFPs. The solid lines are fit to the energy/IMFP values with a Bethe equation (Eq.(3)); the vales of the parameters found in the fit are given in Table 1.

found from a linear least-squares analysis.

The E/λ value can be described as

$$E/\lambda = E_p{}^2 \beta \ln(\gamma E) \qquad \text{.....(3)}$$

Values of the parameters β and γ from the fits are listed in Table 1. The curve fit values (solid lines) are also shown in Fig. 6. In this figure, the experimental data for Au, Ag, and Cu lie close to the straight line over the 50 - 5000 eV energy

Table 1. Values of β and γ found in the fits of the Bethe equation (3) to the experimental IMFPs.
* the value in the parentheses corresponds to the 200 - 5000 eV energy range. R means the correlation coefficient, and rms(%) means the root mean square errors of the curve fit.

Element	β ($eV^{-1}Å^{-1}$)	γ (eV^{-1})	R	rms(%)
Ag	0.0230	0.0316	0.987	10.7
Au	0.0241	0.0380	0.993	7.0
Cu	0.0137	0.0392	0.988	5.9
Si	0.0324	0.0655	0.937	56 (7.0)*

Table 2. IMFPs as a function of electron energy. Those values are calculated from the Bethe formula and the parameters β and γ (in Table 1) which were determined from curve fits to the experimentally determined IMFPs using Fano plots.

Electron energy (eV)	IMFPs (Å) Au	Ag	Cu	Si
50	3.6	5.3	4.2	-
100	3.5	4.3	4.2	-
200	4.6	5.3	5.5	8.7
300	5.7	6.5	6.9	11.3
400	6.8	7.7	8.3	13.7
500	7.9	8.9	9.6	16.1
600	8.9	10.0	10.8	18.3
700	9.9	11.1	12.0	20.5
800	10.9	12.1	13.2	22.7
900	11.8	13.2	14.4	24.8
1000	12.8	14.2	15.5	26.8
1100	13.7	15.2	16.6	28.9
1200	14.6	16.2	17.7	30.9
1300	15.5	17.1	18.8	32.8
1400	16.3	18.1	19.9	34.8
1500	17.2	19.0	21.0	36.7
1600	18.1	20.0	22.0	38.6
1700	18.9	20.9	23.0	40.5
1800	19.8	21.8	24.1	42.3
1900	20.6	22.7	25.1	44.2
2000	21.4	23.6	26.1	46.0
2500	25.5	28.0	31.0	55.0
3000	29.4	32.3	35.8	63.7
3500	33.2	36.4	40.5	72.3
4000	37.0	40.5	45.0	80.6
4500	40.6	44.4	49.5	88.8
5000	44.2	48.4	53.9	96.9

range, and, therefore, equation (3) gave satisfactory results over the entire energy region. On the other hand, the Fano plot for Si did not show the same energy dependence as the other elements. Over 200 eV, however, the experimental points for Si lie close to the straight line. The deviations for energies below 200 eV might be due to the difference of surface electronic excitations to the Ni reference as stated in 3.2. The deviations might also be due to inaccuracies of the elastic-scattering cross sections for these energies.

Table 3. rms(%) difference of IMFPs in Table 2 from those calculated from the Penn algorithm (optical IMFPs) and from the TPP-2M equation over the 200 - 5000 eV energy range.

element	rms(%) difference optical IMFPs	TPP-2M
Au	2.7	3.3
Ag	1.5	4.5
Cu	6.7	1.4
Si	8.3	11.0

Then, the experimental IMFPs, which were calculated from equation(3) and the experimentally determined parameter values in Table 1, are shown in Table 2. We estimated the error range of the experimental IMFPs in Table 2 were 7% for Au, 10% for Ag, 6% for Cu, and 7% for Si based on the standard deviations of the respective curve fits.

The rms differences of the IMFPs in Table 2 from those of optical IMFPs (calculated from energy loss functions using the Penn algorithm [1]) and from the TPP-2M equation are shown in Table 3 for the 200 - 5000 eV energy range. The differences between the experimental IMFPs and the optical and TPP-2M IMFPs are much larger for energies less than 100 eV than for energies higher than 200 eV.(e.g., the Au IMFP is 28 % smaller than that of the optical IMFP at 50 eV, IMFPs of Ag and Cu at 50 eV are less than 13% smaller than those of corresponding optical IMFPs.).

From Table 3, we conclude that the IMFPs of Ag, Au, Cu and Si obtained from elastic peak intensity ratios are in excellent agreement with TPP-2M IMFPs or optical IMFPs for the 200 - 5000 eV energy range.

4. Summary

We have determined IMFPs for Ag, Au, Cu, and Si in the 50 - 5000 eV energy range from backscattered elastic-peak intensities taken by a novel CMA using a Ni reference together with Monte Carlo calculations (Ni reference method). In the Monte Carlo calculations, Thomas-Fermi-Dirac (TFD) potentials were used for the calculation of elastic-scattering cross sections.

The resulting IMFPs of Ag, Au, Cu and Si

from the Ni reference method are in excellent agreement with those calculated from the Penn algorithm, which makes use of experimental optical data and the theoretical Lindhard dielectric function, and from the TPP-2M equation in the 200 - 5000 eV energy range. We conclude that the IMFP ratios of Ag, Au, Cu and Si to Ni, which were calculated from the TPP-2M equation and from the Penn algorithm, are accurate within 10% in this energy range.

We appreciate useful comments and suggestions from Dr. C. J. Powell (NIST).

5. References

[1] D. R. Penn, *Phys. Rev.* **B35**, 482 (1987).
[2] S. Tanuma, C.J. Powell, D.R. Penn, *Surf. Interface Anal.*,**11**, 577(1988).
[3] S. Tanuma, C.J. Powell, D.R. Penn, *Surf. Interface Anal.*,**17**, 911(1991).
[4]S. Tanuma, C.J. Powell, D.R. Penn, *Surf. Interface Anal.*,**17**, 929(1991).
[5] S. Tanuma, C.J. Powell, D.R. Penn, *Surf. Interface Anal.*, **20**, 77(1993).
[6]S. Tanuma, C.J. Powell, D.R. Penn, *Surf. Interface Anal.*,**21**, 165(1994).
[7]S. Tanuma, C.J. Powell, D.R. Penn, *Surf. Interface Anal.*,**25** 25(1997).
[8] G. Gergely, M. Menyhard, K. Pentek, A. Sulyok, A. Jablonski and B. Lesiak, *Vacuum*, **46** (1995) 591
[9] K. Goto, N. Sakakibara, Y. Sakai, *Microbeam Anal.*,**2** (1993) 123.
[10] M. Matsumoto and Y. Kurita, *ACM Trans. on Modeling and Computer Simulation*, **2**(1992)179.
[11] S. Tanuma, S. Ichimura, K. Goto, *Surf. Interface Anal.*,30 (2000)212.